Exploring the prokaryote-eukaryote interplay in microbial mats from an Andean athalassohaline wetland

Carolina F. Cubillos[1*], Pablo Aguilar[2,3,4*], David Moreira[1], Paola Bertolino[1], Miguel Iniesto[1], Cristina Dorador[2,3] and Purificación López-García[1]

[1]Ecologie Systématique Evolution, CNRS, Université Paris-Saclay, AgroParisTech, Gif-sur-Yvette, France

[2]Laboratorio de Complejidad Microbiana, Instituto Antofagasta and Centro de Bioingeniería y Biotecnología (CeBiB), Universidad de Antofagasta, Antofagasta, Chile.

[3]Departamento de Biotecnología, Facultad de Ciencias del Mar y Recursos Biológicos, Universidad de Antofagasta, Antofagasta, Chile

[4]Millennium Nucleus of Austral Invasive Salmonids - INVASAL, Concepción, Chile

*These authors contributed equally

For correspondence: Purificación López-García, puri.lopez@universite-paris-saclay.fr

ABSTRACT

Microbial community assembly results from the interaction between biotic and abiotic factors. However, environmental selection is thought to predominantly shape communities in extreme ecosystems. Salar de Huasco, situated in the high altitude Andean Altiplano, represents a poly-extreme ecosystem displaying spatial gradients of physicochemical conditions. To disentangle the influence of abiotic and biotic factors, we studied prokaryotic and eukaryotic communities from microbial mats and underlying sediments across contrasting areas of this athalassohaline ecosystem. The prokaryotic communities were primarily composed of bacteria, notably including a significant proportion of photosynthetic organisms like Cyanobacteria and anoxygenic photosynthetic members of Alpha- and Gammaproteobacteria and Chloroflexi. Additionally, Bacteroidetes, Verrucomicrobia, and Deltaproteobacteria were abundantly represented. Among eukaryotes, photosynthetic organisms (Ochrophyta, Archaeplastida) were predominant, alongside relatively abundant ciliates, cercozoans, and flagellated fungi. Salinity emerged as a key driver for the assembly of prokaryotic communities. Collectively, abiotic factors influenced both prokaryotic and eukaryotic communities, particularly those of algae. However, prokaryotic communities strongly correlated with photosynthetic eukaryotes, suggesting a pivotal role of biotic interactions in shaping these communities. Co-occurrence networks suggested potential interactions between different organisms, such as diatoms with specific photosynthetic and heterotrophic bacteria or with protist predators, indicating influences beyond environmental selection. While some associations may be explained by environmental preferences, the robust biotic correlations, alongside insights from other ecosystems and experimental studies, suggest that symbiotic and trophic interactions significantly shape microbial mat and sediment microbial communities in this athalassohaline ecosystem.

KEYWORDS: community assembly, microbial mat, extreme environment, bacteria, protist, algae, biotic driver, co-occurrence network

INTRODUCTION

Microbial mats are complex microbial ecosystems that grow on the surface of soils, rocks, or sediments of diverse aquatic habitats (1, 2). These stratified ecosystems accommodate diverse micro-habitats and ecological niches, as well as billions of microorganisms that exhibit wide morphological, phylogenetic and metabolic diversity (2, 3). Microbial mat metabolism integrates autotrophic (notably photosynthetic) and heterotrophic activities related to the progressive degradation of organic matter. These, in turn, strongly depend on steep redox vertical gradients which, as a function of the local hydrochemistry, can sometimes promote mineral precipitation leading to microbialite formation (4-6). Typical metabolic guilds, from surface to depth, broadly include oxygenic photoautotrophs, aerobic heterotrophs, anoxygenic photoautotrophs, sulfide oxidizers, sulfate reducers and methanogens, among others (1, 7, 8). These microbial ecosystems are usually dominated by prokaryotes, which are typically characterized by 16S rRNA gene amplicon sequencing (7, 9). However, the importance of eukaryotes and viruses in microbial mats is being increasingly recognized (e.g. (5, 10-14).

Modern microbial mats are often considered analogues of the oldest recorded ecosystems on Earth (1, 15, 16), such that highly conserved energy and carbon pathways within their anoxic layers can inform about prevailing core metabolism in Precambrian ecosystems (17). Although microbial mats are less widespread now than they were at that time (18), they typically occur worldwide in diverse ecosystems with more or less extreme conditions in terms of salinity, temperature or UV radiation, among others (3, 8, 19). The Andean Plateau (or *´Altiplano´*), in particular, is home to several closed basins harboring wetlands and lagoons, locally called *´salares´*, which are a reservoir of microbial mats thriving under high UV-radiation and exhibiting saline to hypersaline conditions, often combined with high metal content, and extreme daily temperature variation (19, 20). Salar de Huasco, recently declared Natural Park (March 2023), is an athalassohaline ecosystem located at 3,800 m above sea level with high physicochemical spatial variability, notably in terms of salinity. Its aquatic systems range from freshwater to salt-saturated brines, resulting in different microbial habitats as permanent or ephemeral ponds (21, 22). Thus, Salar de Huasco provides an excellent opportunity to study, within close geographic proximity (same basin), how complex microbial communities assemble and vary as a function of local environmental parameters. Several studies have previously focused on the bacteria and archaea thriving in water and/or sediment of different areas in the *salar* (23-26) and, more recently, their viruses (27, 28). In addition to these surveys across space, some temporal studies point out to seasonal variation

(29, 30). Some specific members of these microbial communities have been studied in more detail, such as *Exiguobacterium* sp., which is a halotolerant and arsenic-resistant species isolated from sediment (31-33), or the aerobic anoxygenic phototroph *Rhodobacter* sp. Rb3, isolated from microbial mats (34). However, thorough studies of the microbial mat communities across the *salar* are lacking, as well as information about the microbial eukaryotic component other than fungal spores (35).

In this study, we aimed at identifying the environmental drivers influencing the assembly of both, prokaryotic and eukaryotic communities, from microbial mats and underlying sediment of various sites in the Salar de Huasco with different physicochemical conditions. Our analyses show that both, abiotic and biotic factors, determine microbial community assembly. Specifically, the interplay between prokaryotes and photosynthetic eukaryotes appears remarkably strong.

MATERIALS AND METHODS

Study area, sampling, and measurements of physicochemical parameters

Salar de Huasco (20°18′18 S, 68°50′22 W) includes peatlands (locally called *´bofedales´*), permanent and non-permanent lakes, hypersaline lagoons, and salt crusts (20, 36). Various sampling sites have been historically described within this basin (21), representing gradients from freshwater (e.g., site H0) to hypersaline (e.g., sites H4 and H6) ecosystems. In December 2019 (i.e., during the wet season), we collected microbial mat and sediment samples from four sampling zones (H0, H3, H4, and H6) located in Salar de Huasco (Fig. 1; Table S1). In this study, we denote as microbial mats the upper, layered microbial communities, usually cm-sized (1-5 cm), and as sediments, the undifferentiated, blackish, gray or sandy material underneath the collected microbial mats (5-10 cm depth below the mat). In addition, a biofilm and a water sample were collected from sites H3 and H6, respectively. In total, we studied 19 samples from 11 sampling points distributed in the four sampling zones (Tables S1 and S2). Physicochemical parameters were measured using a multiparameter probe Hanna HI9828 (Table S1).

DNA extraction, PCR amplification and sequencing

Genomic DNA was extracted using the PowerSoil DNA Isolation Kit (MoBio) after the elimination of ethanol and rehydration of the biomass at 4°C for at least 2 h in the resuspension buffer of the kit. DNA was used as a template for the V4-V5 region

amplification (~ 420 bp fragments) of the prokaryotic 16S rRNA with the primer set U515F (5'-GTGCCAGCMGCCGCGGTAA-3') and 926R (5'-CCGYCAATTYMTTTRAGTTT-3'). The eukaryotic 18S rRNA gene V4 region (~527 bp fragments) was amplified using the primers EK-565F (5'-GCAGTTAAAAAGCTCGTAGT-3') and 18S-EUK-1134-R_UNonMet (5'-TTTAAGTTTCAGCCTTGCG-3') biased against metazoans (37). Forward and reverse primers were tagged with 10-bp molecular identifiers (MIDs) to allow pooling and identification of amplicons from different samples. PCR-amplification reactions were performed in 25 µl volume reaction and contained 0.5–3 µl of eluted DNA, 1.5 mM of $MgCl_2$, 0.2 mM of deoxynucleotide (dNTP) mix, 0.3 µM of each primer and 0.5 U of the hot-start Platinum Taq DNA Polymerase (Invitrogen, Carlsbad, CA). PCR reactions were carried out for 35 cycles (94°C for 30 s, 55–58°C for 30–45 s, 72°C for 90 s) preceded by 2 min denaturation at 94°C and followed by five additional minutes of polymerization at 72°C. To minimize PCR bias, five different PCR reactions were pooled for each sample. Amplicons were then purified using the QIAquick PCR purification kit (Qiagen, Hilden, Germany). Sequencing was done using Illumina Miseq (2x300 bp, paired-end) at Eurofins Genomics (Konstanz, Germany). Sequence data are available 16S rRNA gene amplicon Illumina sequences have been deposited in the GenBank (NCBI) Short Read Archive with BioProject number PRJNA1046993.

Amplicon data processing

1,585,086 raw sequences (reads) for 16S and 18S rDNA amplicons were obtained from 19 samples. The raw reads were analyzed using QIIME2 v.2020.8 (38). Briefly, the reads were demultiplexed using the "cutadapt demux-paired" function, and then, the DADA2 plugin was used to determine amplicon sequence variants (ASVs) after denoising, dereplication, and chimera-filtering (39). The optimal truncation parameters were selected using the program FIGARO (40). The forward and reverse reads were merged to obtain complete denoised ASV sequences. Denoised sequences with one or more mismatches in the overlap region were removed. Sequence and ASV statistics are provided in Table S2). ASVs were assigned to archaeal and bacterial taxa, based on the GTDB taxonomy (https://gtdb.ecogenomic.org/) release 207, using an in-house qiime classifier, which was trained and tested following qiime documentation (function feature-classifier) for prokaryotes; The curated database PR2 was used for eukaryotes (41). After the quality-filtering process, a total of 9,135 prokaryotic ASVs were obtained, 565 of which were archaeal ASVs. A total of 1,715 eukaryotic ASVs were determined across all samples. Sequences affiliating to chloroplasts, mitochondria and

Metazoa were removed from the analysis. The relative abundance and taxonomic affiliation of ASVs are provided in Table S3 and Table S4, respectively.

Diversity, statistical, and network analyses

The estimates of species richness, Simpson, Shannon-wiener, and Pielou's diversity indexes were calculated using the "diversity alpha" function implemented in QIIME2 v.2020.8 (Table S2). Bray–Curtis distance (based on the relative abundance –percentage– of ASVs), ordinations (Non-Metric Multidimensional Scaling –NMDS– using the function metaMDS), the fit of environmental vectors into ordinations, and statistical differences among samples (ANOSIM) were calculated using the Vegan package in R (R Core Team, 2018; Oksanen *et al.*, 2019). To test whether the prokaryotic community was significantly correlated to the environmental variables and the eukaryotic community, we carried out Mantel tests using Spearman's correlation on the Bray-Curtis distance matrix and a matrix of Euclidean distances of the measured physicochemical parameters. To identify the core microbiome (i.e., microbial taxa shared by microbial mats and their underlying sediments) we used the package microbiome (DOI:10.18129/B9.bioc.microbiome) in R (42) applying an abundance-occurrence method with a threshold detection of 0.1% of relative abundance and persistence of 50%. We carried out a co-occurrence network analysis included prokaryotic and eukaryotic ASVs from mat and underlying sediment samples. The network was constructed using Spearman's correlation and SpiecEasi with the Meinshausen and Bühlmann (mb) method (43). Negative edges (n=464) were removed to visualize only co-occurrences, and edges were further filtered to exclusively show prokaryote—eukaryote co-occurrences. Additionally, we applied cut-off threshold to avoid spurious correlations, keeping only the top 30% edges positively correlated were retained. We used the fast-greedy clustering algorithm to detect clusters within the networks (44) and removed clusters with less than 4 nodes. In addition, the network topology measurements were calculated, including node and edge number, number of clusters, diameter, and modularity (Table S5). The network was visualized with the igraph R package (45).

RESULTS AND DISCUSSION

Alpha diversity of prokaryotic and eukaryotic communities

We studied the diversity of prokaryotes and microbial eukaryotes in microbial mats and underlying sediment (17 samples) from four major zones classically studied in the Salar de

Huasco; two additional samples corresponded to plankton and one biofilm. These zones (H0 to H4) exhibit different physicochemical parameters (23, 24). Notably, at the sampling time, pH varied between 7 and 9, and salinity between 0.2 and 18.9 PSU (Table S1). The low salinity was associated to water inflow points in the *salar*. We observed a general salinity increase trend from the H0 zone, which is the main freshwater entry point, to the H4 zone, consistent with previous studies (24, 27). However, we also observed a high spatial heterogeneity, as has also been previously noted in Salar de Huasco (24, 29) and other high-altitude salt flats (46, 47). Thus, different points in the H4 zone exhibited different salinity values and, most notably, different sampling points had radically different levels of dissolved oxygen (Table S1). This variation from complete anoxia to highly oxic waters was related to the size and level of confinement of the different ponds, with smaller, deep ponds, being sometimes oxygen deprived.

We massively sequenced 16S and 18S rRNA gene amplicons to characterize, respectively, the prokaryotic (archaeal + bacterial) and eukaryotic diversity associated to these samples. We generated ASVs that were used to derive alpha diversity metrics (Table S2). The highest diversity values corresponded, as expected, to the prokaryotic component, with bacteria being prevalent. Thus, from the total 9,135 prokaryotic ASVs identified, 565 were archaeal. Only a small subset of those ASVs (2,864 bacterial, 38 archaeal) were shared between samples, which attests to the high heterogeneity of the different samples. From the total 1,715 eukaryotic ASVs identified, 570 were shared across samples; this higher percentage of shared ASVs was partly due to the occurrence of motile predatory protists (see below). Alpha diversity metrics for prokaryotes were not significantly different across samples (Shapiro-Wilk test, $p > 0.05$). However, the Simpson and Shannon-Wiener diversity indices, as well as Pielou's index (evenness) were significantly different (Shapiro-Wilk test, $p < 0.05$) between sample types, with higher values in the sediments as compared to the layered microbial mats on top of those sediments. The alpha diversity values for the eukaryotic microbial community were also higher for sediments, although the difference with other sample types was not significant (Shapiro-Wilk test, $p > 0.05$). We observed similar trends for prokaryotes and microbial eukaryotes when comparing among sampling sites.

Prokaryotic and eukaryotic components of microbial communities

To get a phylogenetic insight into the microbial community structure of microbial mats and the underneath sediment, we attributed the ASVs to different taxa and determined relative abundances (Tables S3 and S4). One biofilm floating in one of the ponds (H3.1.BF) and one

plankton sample (H6.3.W.CT) were included for comparison (Table S2; Fig. 2). Bacteria largely dominated prokaryotic communities across samples (mean relative abundance of 96.2%), archaea representing the remaining, minor fraction of the community (Fig. 2A).

Overall, the most abundant bacterial high-rank taxa were the Bacteroidota (up to 41.8% of relative abundance), Alphaproteobacteria (up to 24.4%), and Gammaproteobacteria (up to 13.8%). However, their mean relative abundance in mat and sediment samples differed, as expected. Bacteroidota (29.8%), Alphaproteobacteria (15.1%), Gammaproteobacteria (11.1%), Cyanobacteria (8.3%), and Verrucomicrobia (4.1%) were more abundant in the microbial mat samples. This distribution is consistent with the major metabolic functions associated to the two compartments. In the Salar de Huasco microbial mats, the photosynthetic cyanobacteria but also the anoxygenic photosynthetic members of the Alpha- and Gammaproteobacteria (essentially Rhodobacterales and Chromatiales, respectively) and, to a lesser extent, members of the Chloroflexales (Table S3 and Fig. S1), contribute to the primary production. Even some members of the consistently present but relatively low abundant Gemmatimonadota might include photosynthetic representatives (48, 49). The Bacteroidota were highly diverse and integrated only typical heterotrophic members of major classes Bacteroidia (Bacteroidales, Flavobacteriales, Chytinophagales, Sphingobacteriales), Kapabacteria, Ignavibacteria and Rhodothermia, among others (Fig. S1). They are most likely involved in the degradation of biopolymers produced by cyanobacteria and other photosynthetic members of the community. Bacteroidetes are well known for containing a wide diversity of enzymes to degrade glycans (50) (51), being typically associated to microbial mats (5, 46, 52, 53) and other carbohydrate-rich environments, including animal guts (54). Actually, some Chytinophagales positively correlate with green algal production (55) and some Ignavibacteria are known to be specifically cellulolytic (56). Some Kapabacteria seem to include potential sulfate reducers (57) and, accordingly, might potentially be responsible for the reduction of oxidized sulfur compounds produced by the sulfide-reducing members of the alpha- and gammaproteobacterial photosynthesizers in the microbial mat compartment.

Although Bacteroidota and Alpha- and Gammaproteobacteria were also abundant in sediments, their proportion diminished as compared with the upper microbial mat layers, while heterotrophic members of the Chlorofexota (11.3%), Deltaproteobacteria (mostly Desulfobacterota, Bdellovibrionota and Myxococcota; 9.4%) and Patescibacteria (2.8%) displayed higher relative abundances (Fig. 2A; Fig. S1). Patescibacteria were particularly abundant in the plankton sample (~20%). This bacterial taxon is highly diverse and comprises

epibiotic, likely parasitic, bacteria (58). Frequent in subsurface waters, these bacteria seem more driven by host availability than environmental parameters (59, 60). Some Patescibacteria prey on photosynthetic gammaproteobacteria, such as *Vampirococcus lugosii* (Absconditabacterales) (61). Given the relative abundance of these type of anoxygenic photosynthesizers, they might be a potential target for some members of that patescibacterial order (Table S3). Deltaproteobacterial taxa, including among other newly defined phyla the Desulfobacterota, Bdellovibrionota and Myxococcota, are typically associated to microbial mat layers and sediments. Many Desulfobacterota are typical sulfate reducers that participate in the degradation of organics and the sulfur cycle (62), although others, are involved in hydrogen-mediated syntrophy (63). Bdellovibrionota and Myxococcota are known as typical bacterial predators (64), although they might even occasionally contribute to photosynthetic carbon fixation (65).

The archaeal community was dominated by Nanoarchaeota and Thermoplasmatota, which reached the highest mean proportion in sediment samples (4.2% and 1%, respectively), although Nanoarchaeota reached values around up to 10-13% in the sediment samples H0.1.S, H6.1.S.5.10cm and the plankton sample (Fig. 2A). Pacearchaeales and Woesearchaeales were the most abundant groups in these three samples (Fig. S1). The rest of the archaea were diverse across samples, albeit less relatively abundant, and comprised Thermoplasmatota (essentially the groups DHVEG-1, EX4484-6, SG8-5, and UBA10834), Halobacteriota (Halobacteriales, Methanomicrobiales, Methanosarcinales, and Methanotrichales), Thermoproteota (B26-1), and Asgardarchaeota (Lokiarchaeles, Helarchaeales, and Thorarchaeales) (Fig. S1).

The eukaryotic community was largely dominated by Ochrophyta (up to 87% of the protist component) in almost all samples (Fig. 2B). This group of photosynthetic stramenopiles included pennate diatoms (Bacillariophyta), golden algae (Chrysophyceae), yellow-green algae (Xantophyceae) and one Dyctiochophyceae ASV (Table S4; Fig. S2). Among the Archaeplastida, green algae (Chlorophyta) and Streptophyta were rather abundant, with minor occurrences of red algae (Rhodophyta). Rare Cryptophyta and Haptophyta ASVs completed the photosynthetic cohort of microbial eukaryotes in the Salar de Huasco samples. These groups were not only detected in the microbial mats but also in the underlying sediments, indicating that, although they can no longer perform photosynthesis, their DNA is preserved during burial. Diatom DNA appears to be particularly well preserved in ancient samples and can be used to retrace historical events (66). Ciliates, fungi and Cercozoa were the three more represented clades of heterotrophic eukaryotes. Ciliates were

highly diverse, although the most represented groups were the Oxytrichidae and Sessilida (Table S4). Ciliates are usually abundant grazers feeding on benthic samples and are typically identified on microbial mats and freshwater systems (5, 67). Fungi were dominated by flagellated lineages (68), many of which may be parasites of other opisthokonts. Cercozoans comprised diverse lineages of predators including vampyrellids (Fig. S2), some of which are typical predators of algal lineages (69) and members of the clade 10-12, which are eukaryvorous flagellates widespread in freshwater systems (70).

We looked for shared ASVs potentially conforming a core microbiome in microbial mats and sediments. The prokaryotic core microbiome across space and sample types was small: 11 ASVs for microbial mats and 30 ASVs for sediments (Fig. S3). Four ASVs corresponded to photosynthetic genera in microbial mats, one alphaproteobacterium (Rhodobacteraceae), two gammaproteobacteria (genus *Thioploca*) and one cyanobacterium belonging to the genus *Symploca*. The latter genus groups cyanobacteria producing highly cytotoxic compounds (71), which might perhaps facilitate its colonization across samples. The prokaryotic sediment core comprised members of the Bacteroidota, Chloroflexota, Cyanobacteria, Gammaproteobacteria, Alphaproteobacteria, Deltaproteobacteria, Firmicutes, Spirochaetota, and Gemmatimonadota (Fig. S3). The protist core microbiome was also very limited. In microbial mats, it involved two diatom and two ciliate ASVs; in the sediments, 11 diatom ASVs and one fungal ASV (Fig. S3). Overall, this reduced core of shared ASVs illustrated sample heterogeneity and suggested strong local environmental selection.

Environmental drivers of prokaryotic and eukaryotic community assembly

Both abiotic and biotic factors contribute to microbial community assembly (72). In extreme environments, environmental selection is thought to play a key role but the influence of biotic interactions has been rarely studied in this type of systems. In our study, we tried to disentangle the influence of abiotic versus biotic factors on prokaryotic and eukaryotic members of the Salar de Huasco microbial communities. To do so, we first looked for the effect of the measured physicochemical parameters on community structure. Ordination analyses (NMDS) of prokaryotic and eukaryotes communities showed relatively dispersed communities, even though samples from the same sampling zone tended to group together (Fig. 3). We applied ANOSIM tests to see whether microbial communities significantly differed among samples. This was the case for prokaryotic communities, which differed among sampling sites (ANOSIM, R = 0.3, p = 0.01) and sample types (ANOSIM, R = 0.24, p = 0.02). Furthermore, prokaryotic communities segregated according to the salinity gradient

exhibited across sampling sites (Fig. 3A). Salinity (R^2 = 0.4) and the related parameters, total dissolved solids (TDS; R^2 = 0.57) and electrical conductivity (R^2 = 0.55), had a significant effect on the segregation of the prokaryotic fraction. By contrast, global eukaryotic communities did not show significant differences across sampling sites (R = 0.13, p = 0.15) or sample types (R = 0.07, p = 0.26). However, pH appeared to explain, albeit with modest probability (R^2 = 0.35, p = 0.041), the distribution of eukaryotic communities on the ordination analysis (Fig. 3B).

We then looked for the cumulative effect of measured environmental factors (Table S1) on the community structure, measured via Bray-Curtis distances, both for prokaryotes and eukaryotes, using Mantel tests. We excluded dissolved oxygen, which was only measured in the water column above the mat and sediment samples. Taken together, these abiotic factors significantly correlated with prokaryotic and eukaryotic components of microbial communities, although the correlation was stronger for prokaryotes (Fig. 4A) than for eukaryotes (Fig. 4B). Since motile predatory protists, such as ciliates or cercozoans, which can move between sites and are not strictly associated to benthic communities, constituted a considerable fraction of the eukaryotic communities, we also carried out independent tests for photosynthetic and non-photosynthetic eukaryotes. While algal communities showed a significant, albeit weak, correlation with environmental parameters (Fig. 4C), heterotrophic eukaryotes, as expected, did not correlate with differences of abiotic parameters across Huasco sites (Fig. 4D).

Finally, we looked for a potential mutual influence of prokaryotic and eukaryotic communities. Mantel tests showed a marked significant correlation of prokaryotic communities and both, photosynthetic (Fig. 4E) and non-photosynthetic (Fig. 4F) eukaryotes. However, the correlation of prokaryotes with heterotrophic eukaryotes was somewhat weaker and apparently driven by some outlier points (Fig. 4F). By contrast, the correlation of prokaryotes and benthic algae was much stronger and even (Fig. 4E), suggesting a strong interplay between these two components of microbial communities across Salar de Huasco samples.

Co-occurring patterns in mat and sediment communities

To identify more specific potential interactions between prokaryotes and eukaryotes in microbial mats and sediments, we built co-occurrence networks. The global co-occurrence network was complex (Fig. S4) and, to facilitate the visualization of inter-domain co-occurring ASVs, we filtered out negative correlations and retained only the top 30% positive

correlations that contained both eukaryotes and prokaryotes (Fig. 5). This network consisted of 116 nodes (69 bacterial, 47 eukaryotic; Table S5-S6). Without surprise, archaeal nodes were not identified under the chosen filters. Using a fast greedy algorithm, we identified 19 clusters within the co-occurring network. Eukaryotes, essentially Ochrophyta, displayed the highest number of edges in 9 clusters, whereas bacteria, notably Proteobacteria, were central in only 3 clusters (Fig. 5; Table S6).

While some co-occurrences might be due to similar preferences for specific environmental conditions, some might actually reflect trophic or symbiotic (mutualistic, commensal or parasitic) interactions. In many cases, disentangling the two possibilities (environmental preference versus biotic interactions) will require experimental evidence; yet, identifying these potential interactions may orient further studies. The stronger correlation between prokaryotes and photosynthetic eukaryotes (Fig. 4E) indeed suggested a role for biotic interactions. In Salar de Huasco, diatoms were the most represented ochrophytes and they co-occurred with cyanobacteria and their typically associated glycan-degrading Bacteroidota in several clusters, notably clusters 3, 5 and 11. Diatoms might co-occur with cyanobacteria because they need light and similar specific conditions. However, symbioses between diatoms and N_2-fixing cyanobacteria are widespread in marine and other ecosystems (73, 74), suggesting that this type of mutualisms might be operational in Huasco as well. Some of the cyanobacterial ASVs co-occurring with diatoms were not assigned to described genera and it is difficult to predict whether they represent N_2-fixers, especially since N_2 fixation, although widespread, is patchily distributed among cyanobacterial taxa (75). However, some ASVs could be assigned to known genera of N_2-fixers, such as *Dolichospermum*, which co-occurs with diatoms in cluster 11 (76) (Tables S6; Fig. 5). Furthermore, N_2 fixation is not exclusive of cyanobacterial communities but can also be carried out by some anoxygenic phototrophs (e.g. several Proteobacteria and Chlorobi) in their respective (micro)oxic and anoxic microbial mat niches (77), therefore bearing a potential for metabolic exchange with diatoms. Thus, different clusters associated diatoms with anoxygenic photosynthetic proteobacteria, e.g. cluster 1 and cluster 10, the latter including *Thiocapsa*, a genus also bearing N_2 fixers (78). Gemmatimonadetes, which also comprise some phototrophic organisms (79), were also often associated to diatoms (clusters 4, 12, 14 or 17). Interestingly, these bacteria can attach to diatoms in the epilimnion of some lakes (80).

In addition to potential symbiotic interactions, some of the observed co-occurrences might reflect trophic interactions and prey preferences. For instance, ciliates and some

amoeba (lobosa, conosa) were frequently associated to Proteobacteria and Bacteroidota or Cyanobacteria (cluster 13 and 18). Some other algal predatory protists, such as vampyrellids (81), occurred in clusters containing diatoms or other ochrophytes (Clusters 5, 6 and16). Desulfobacterota appeared also in several clusters (Fig. 5). In summary, at finer taxonomic levels, our study suggests that, beyond the threshold of environmental selection, several specific trophic and symbiotic interactions shape Salar de Huasco microbial mat and sediment communities.

Concluding remarks

Both abiotic and biotic factors contribute to microbial community assembly (72). However, for microbial communities, environmental selection by abiotic parameters is often thought to be determinant since early times and the "*everything is everywhere but the environment selects*" tenet from the Delft's school of microbiology (82, 83). Thus, environmental selection is thought to be dominant especially for extreme environments such as deserts, hypersaline or hot settings, where abiotic selective pressures are strong (e.g. (84-87). Nonetheless, on top of a potential role of stochasticity (88), it is becoming clear that functional selection imposed by other community members (89, 90) and other trophic interactions (91), which may take place at very small scale (92), are also key drivers of microbial community assembly (91). Here, we tried to disentangle the influence of abiotic versus biotic factors on prokaryotic and eukaryotic members of microbial mats and underlying sediments in the Salar de Huasco, which qualifies as a poly-extreme extreme environment and exhibits spatial physicochemical gradients (21, 22) (20). 16S/18S rRNA gene amplicon studies revealed widely diverse prokaryotic, and to a lesser extent, eukaryotic communities. The photosynthetic component of these communities was particularly abundant and diverse, with both oxygenic (cyanobacteria, and eukaryotic algae – essentially ochrophytes and Archaeplastida) and anoxygenic photosynthesizers (several Alpha- and Gammaproteobacteria and Chloroflexi). Despite the presence of the similar high-rank taxa (Fig. 2), lower-rank taxa (ASVs) differed among sites, with very reduced core prokaryotic and eukaryotic microbiomes, suggesting strong local environmental selection. In particular, salinity influenced the most prokaryotic community assembly (Fig. 3). Globally, the cumulated effect of measured environmental parameters significantly correlated with prokaryotic and protist communities. However, within eukaryotes, we observed a marked difference between the photosynthetic and the heterotrophic fraction, the latter not displaying any significant correlation with the environmental factors (Fig. 4). Benthic algae, little or no motile, seemed to be shaped by the

local physicochemistry and behave very much like the prokaryotic component of microbial mats and sediments. By contrast, heterotrophic protists, such as ciliates, amoeba and cercozoans, are flexible grazers able to move between different areas in the Salar. Interestingly, the influence of biotic factors seemed to be much higher than that of abiotic parameters. In particular, prokaryotic communities strongly correlated with photosynthetic eukaryotes (Fig. 4). Co-occurrence networks suggest potential interactions between specific community members, for instance between diatoms and specific photosynthetic and heterotrophic bacteria, or protist predators. While this influence could be partly explained by similar environmental preference, the strong biotic correlation together with known interactions from similar partners in other ecosystems (73, 74, 80, 81), suggest that symbiotic (from mutualism to parasitism) and trophic and interactions shape the microbial mat and sediment communities in this athalassohaline ecosystem. Our study highlights the importance of considering the entire microbial community, including eukaryotic microorganisms, to better understand community assembly. Further studies focusing on the functional role of specific microbial interactions should provide deeper insights into the microbial ecology of the Salar de Huasco and other similar athalassohaline systems. The knowledge gained from the Andean Altiplano *salares*, severly threatened by mining activities (93), can also aid in preserving these unique microbial ecosystems.

ACKNOWLEDGEMENTS

This work was supported by the bilateral French-Chilean ECOS Sud-ANID cooperation program (project MMEX), the ERC AdG PlastEvol (787904, DM) and the Moore-Simons Project on the Origin of the Eukaryotic Cell, Moore Foundation grant GBMF9739 (PL-G; https://doi.org/10.37807/GBMF9739). PA received funding from ANID – Millennium Science Initiative Program – NCN2021-056.

REFERENCES

1. Des Marais DJ. 1990. Microbial mats and the early evolution of life. Trends Ecol Evol 5:140-144.
2. Stal LJ. 2012. Cyanobacterial mats and stromatolites, p 65–125. *In* Whitton BA (ed), Ecology of cyanobacteria II. Springer Netherlands, Dordrecht.

3. Prieto-Barajas CM, Valencia-Cantero E, Santoyo G. 2018. Microbial mat ecosystems: Structure types, functional diversity, and biotechnological application. Electronic Journal of Biotechnology 31:48-56.
4. Dupraz C, Visscher PT. 2005. Microbial lithification in marine stromatolites and hypersaline mats. Trends Microbiol 13:429-438.
5. Iniesto M, Moreira D, Reboul G, Deschamps P, Benzerara K, Bertolino P, Saghaï A, Tavera R, López-García P. 2021. Core microbial communities of lacustrine microbialites sampled along an alkalinity gradient. Environ Microbiol 23:51-68.
6. Caumartin J, Benzerara K, Havas R, Thomazo C, Lòpez-García P, Duprat E. 2023. The chemical conditions necessary for the formation of microbialites. Geochemical Perspectives Letters 25:30-35.
7. Ley RE, Harris JK, Wilcox J, Spear JR, Miller SR, Bebout BM, Maresca JA, Bryant DA, Sogin ML, Pace NR. 2006. Unexpected diversity and complexity of the Guerrero Negro hypersaline microbial mat. Appl Environ Microbiol 72:3685-3695.
8. Bolhuis H, Cretoiu MS, Stal LJ. 2014. Molecular ecology of microbial mats. FEMS Microbiol Ecol 90:335-350.
9. Robertson CE, Spear JR, Harris JK, Pace NR. 2009. Diversity and stratification of archaea in a hypersaline microbial mat. Appl Environ Microbiol 75:1801-1810.
10. Saghaï A, Gutierrez-Preciado A, Deschamps P, Moreira D, Bertolino P, Ragon M, Lopez-Garcia P. 2017. Unveiling microbial interactions in stratified mat communities from a warm saline shallow pond. Environ Microbiol 19:2405-2421.
11. Carreira C, Staal M, Middelboe M, Brussaard CPD. 2015. Counting Viruses and Bacteria in Photosynthetic Microbial Mats. Appl Environ Microbiol 81:2149-2155.
12. Carreira C, Lønborg C, Kühl M, Lillebø AI, Sandaa R-A, Villanueva L, Cruz S. 2020. Fungi and viruses as important players in microbial mats. FEMS Microbiol Ecol 96.
13. White RA, 3rd, Visscher PT, Burns BP. 2021. Between a Rock and a Soft Place: The Role of Viruses in Lithification of Modern Microbial Mats. Trends Microbiol 29:204-213.
14. López-García P, Gutiérrez-Preciado A, Krupovic M, Ciobanu M, Deschamps P, Jardillier L, López-Pérez M, Rodríguez-Valera F, Moreira D. 2023. Metagenome-derived virus-microbe ratios across ecosystems. ISME J 17:1552–156.
15. Margulis L, Barghoorn ES, Ashendorf D, Banerjee S, Chase D, Francis S, Giovannoni S, Stolz J. 1980. The microbial community in the layered sediments at Laguna Figueroa,

Baja California, Mexico: Does it have Precambrian analogues? Precambrian research 11:93-123.

16. Noffke N, Eriksson KA, Hazen RM, Simpson EL. 2006. A new window into Early Archean life: Microbial mats in Earth's oldest siliciclastic tidal deposits (3.2 Ga Moodies Group, South Africa). Geology 34:253.
17. Gutierrez-Preciado A, Saghai A, Moreira D, Zivanovic Y, Deschamps P, Lopez-Garcia P. 2018. Functional shifts in microbial mats recapitulate early Earth metabolic transitions. Nat Ecol Evol 2:1700-1708.
18. Allwood AC, Walter MR, Kamber BS, Marshall CP, Burch IW. 2006. Stromatolite reef from the Early Archaean era of Australia. Nature 441:714-718.
19. Farías ME, Saona Acuña LA. 2020. Modern microbial mats and endoevaporite systems in andean lakes: A general approach, p 21-33. *In* Farías ME (ed), Microbial ecosystems in central andes extreme environments: biofilms, microbial mats, microbialites and endoevaporites doi:10.1007/978-3-030-36192-1_2. Springer International Publishing, Cham.
20. Dorador C, Molina V, Hengst M, Eissler Y, Cornejo M, Fernández C, Pérez V. 2020. Microbial communities composition, activity, and dynamics at salar de huasco: A polyextreme environment in the chilean altiplano, p 123–139. *In* Farías ME (ed), Microbial ecosystems in central andes extreme environments: biofilms, microbial mats, microbialites and endoevaporites. Springer International Publishing, Cham.
21. Dorador C, Busekow A, Vila I, Imhoff JF, Witzel K-P. 2008. Molecular analysis of enrichment cultures of ammonia oxidizers from the Salar de Huasco, a high altitude saline wetland in northern Chile. Extremophiles: Life Under Extreme Conditions 12:405-414.
22. Aguilar P, Acosta E, Dorador C, Sommaruga R. 2016. Large Differences in Bacterial Community Composition among Three Nearby Extreme Waterbodies of the High Andean Plateau. Front Microbiol 7:976.
23. Dorador C, Vila I, Remonsellez F, Imhoff JF, Witzel KP. 2010. Unique clusters of Archaea in Salar de Huasco, an athalassohaline evaporitic basin of the Chilean Altiplano. FEMS Microbiol Ecol 73:291-302.
24. Hernández KL, Yannicelli B, Olsen LM, Dorador C, Menschel EJ, Molina V, Remonsellez F, Hengst MB, Jeffrey WH. 2016. Microbial Activity Response to Solar Radiation across Contrasting Environmental Conditions in Salar de Huasco, Northern Chilean Altiplano. Front Microbiol 7:1857.

25. Castro-Severyn J, Pardo-Esté C, Mendez KN, Fortt J, Marquez S, Molina F, Castro-Nallar E, Remonsellez F, Saavedra CP. 2021. Living to the High Extreme: Unraveling the Composition, Structure, and Functional Insights of Bacterial Communities Thriving in the Arsenic-Rich Salar de Huasco Altiplanic Ecosystem. Microbiol Spectr 9:e0044421.
26. Corona Ramírez A, Cailleau G, Fatton M, Dorador C, Junier P. 2022. Diversity of Lysis-Resistant Bacteria and Archaea in the Polyextreme Environment of Salar de Huasco. Front Microbiol 13:826117.
27. Eissler Y, Gálvez MJ, Dorador C, Hengst M, Molina V. 2019. Active microbiome structure and its association with environmental factors and viruses at different aquatic sites of a high-altitude wetland. Microbiologyopen 8:e00667.
28. Eissler Y, Dorador C, Kieft B, Molina V, Hengst M. 2020. Virus and Potential Host Microbes from Viral-Enriched Metagenomic Characterization in the High-Altitude Wetland, Salar de Huasco, Chile. Microorganisms 8.
29. Paquis P, Hengst MB, Florez JZ, Tapia J, Molina V, Pérez V, Pardo-Esté C. 2023. Short-term characterisation of climatic-environmental variables and microbial community diversity in a high-altitude Andean wetland (Salar de Huasco, Chile). Sci Total Environ 859:160291.
30. Pardo-Esté C, Leiva SG, Remonsellez F, Castro-Nallar E, Castro-Severyn J, Saavedra CP. 2023. Exploring the Influence of Small-Scale Geographical and Seasonal Variations Over the Microbial Diversity in a Poly-extreme Athalosaline Wetland. Curr Microbiol 80:297.
31. Remonsellez F, Castro-Severyn J, Pardo-Esté C, Aguilar P, Fortt J, Salinas C, Barahona S, León J, Fuentes B, Areche C, Hernández KL, Aguayo D, Saavedra CP. 2018. Characterization and Salt Response in Recurrent Halotolerant Exiguobacterium sp. SH31 Isolated From Sediments of Salar de Huasco, Chilean Altiplano. Front Microbiol 9:2228.
32. Castro-Severyn J, Pardo-Esté C, Mendez KN, Morales N, Marquez SL, Molina F, Remonsellez F, Castro-Nallar E, Saavedra CP. 2020. Genomic Variation and Arsenic Tolerance Emerged as Niche Specific Adaptations by Different Exiguobacterium Strains Isolated From the Extreme Salar de Huasco Environment in Chilean - Altiplano. Front Microbiol 11:1632.
33. Castro-Severyn J, Pardo-Esté C, Araya-Durán I, Gariazzo V, Cabezas C, Valdés J, Remonsellez F, Saavedra CP. 2022. Biochemical, genomic and structural characteristics

of the Acr3 pump in Exiguobacterium strains isolated from arsenic-rich Salar de Huasco sediments. Front Microbiol 13:1047283.

34. Perez V, Dorador C, Molina V, Yanez C, Hengst M. 2018. Rhodobacter sp. Rb3, an aerobic anoxygenic phototroph which thrives in the polyextreme ecosystem of the Salar de Huasco, in the Chilean Altiplano. Antonie Van Leeuwenhoek 111:1449-1465.
35. Corona Ramirez A, Bregnard D, Junier T, Cailleau G, Dorador C, Bindschedler S, Junier P. 2023. Assessment of fungal spores and spore-like diversity in environmental samples by targeted lysis. BMC Microbiol 23:68.
36. Risacher F, Alonso H, Salazar C. 2003. The origin of brines and salts in Chilean salars: a hydrochemical review. Earth-Science Reviews 63:249-293.
37. Bower SM, Carnegie RB, Goh B, Jones SRM, Lowe GJ, Mak MWS. 2004. Preferential PCR amplification of parasitic protistan small subunit rDNA from metazoan tissues. J Euk Microbiol 51:325-332.
38. Bolyen E, Rideout JR, Dillon MR, Bokulich NA, Abnet CC, Al-Ghalith GA, Alexander H, Alm EJ, Arumugam M, Asnicar F, Bai Y, Bisanz JE, Bittinger K, Brejnrod A, Brislawn CJ, Brown CT, Callahan BJ, Caraballo-Rodríguez AM, Chase J, Cope EK, Da Silva R, Diener C, Dorrestein PC, Douglas GM, Durall DM, Duvallet C, Edwardson CF, Ernst M, Estaki M, Fouquier J, Gauglitz JM, Gibbons SM, Gibson DL, Gonzalez A, Gorlick K, Guo J, Hillmann B, Holmes S, Holste H, Huttenhower C, Huttley GA, Janssen S, Jarmusch AK, Jiang L, Kaehler BD, Kang KB, Keefe CR, Keim P, Kelley ST, Knights D, et al. 2019. Reproducible, interactive, scalable and extensible microbiome data science using QIIME 2. Nat Biotechnol 37:852-857.
39. Callahan BJ, McMurdie PJ, Rosen MJ, Han AW, Johnson AJA, Holmes SP. 2016. DADA2: High-resolution sample inference from Illumina amplicon data. Nature Methods 13:581-583.
40. Sasada R, Weinstein M, Prem A, Jin M, Bhasin J. 2020. FIGARO: An efficient and objective tool for optimizing microbiome rRNA gene trimming parameters. Journal of Biomolecular Techniques : JBT 31:S2-S2.
41. Guillou L, Bachar D, Audic S, Bass D, Berney C, Bittner L, Boutte C, Burgaud G, de Vargas C, Decelle J, Del Campo J, Dolan JR, Dunthorn M, Edvardsen B, Holzmann M, Kooistra WH, Lara E, Le Bescot N, Logares R, Mahe F, Massana R, Montresor M, Morard R, Not F, Pawlowski J, Probert I, Sauvadet AL, Siano R, Stoeck T, Vaulot D, Zimmermann P, Christen R. 2013. The Protist Ribosomal Reference database (PR2): a

catalog of unicellular eukaryote Small Sub-Unit rRNA sequences with curated taxonomy. Nucleic Acids Res 41:D597-D604.

42. R Development Core Team. 2017. R: A language and environment for statistical computing., vhttp://www.r-project.org. R Foundation for Statistical Computing, Vienna, Austria.
43. Meinshausen N, Bühlmann P. 2006. High-dimensional graphs and variable selection with the Lasso. The Annals of Statistics 34:1436-1462.
44. Clauset A, Newman MEJ, Moore C. 2004. Finding community structure in very large networks. Physical Review E 70.
45. Csardi G, Nepusz T. 2006. The igraph software package for complex network research. InterJournal, Complex Systems 1695:1-9.
46. Dorador C, Fink P, Hengst M, Icaza G, Villalobos AS, Vejar D, Meneses D, Zadjelovic V, Burmann L, Moelzner J, Harrod C. 2018. Microbial community composition and trophic role along a marked salinity gradient in Laguna Puilar, Salar de Atacama, Chile. Antonie Van Leeuwenhoek 111:1361-1374.
47. Demergasso C, Escudero L, Casamayor EO, Chong G, Balague V, Pedros-Alio C. 2008. Novelty and spatio-temporal heterogeneity in the bacterial diversity of hypersaline Lake Tebenquiche (Salar de Atacama). Extremophiles 12:491-504.
48. Zeng Y, Baumbach J, Barbosa EG, Azevedo V, Zhang C, Koblížek M. 2016. Metagenomic evidence for the presence of phototrophic Gemmatimonadetes bacteria in diverse environments. Environ Microbiol Rep 8:139-49.
49. Zeng Y, Feng F, Medová H, Dean J, Koblížek M. 2014. Functional type 2 photosynthetic reaction centers found in the rare bacterial phylum Gemmatimonadetes. Proc Natl Acad Sci U S A 111:7795-800.
50. Lapébie P, Lombard V, Drula E, Terrapon N, Henrissat B. 2019. Bacteroidetes use thousands of enzyme combinations to break down glycans. Nat Commun 10:2043.
51. Larsbrink J, McKee LS. 2020. Bacteroidetes bacteria in the soil: Glycan acquisition, enzyme secretion, and gliding motility. Adv Appl Microbiol 110:63-98.
52. Saghaï A, Zivanovic Y, Moreira D, Benzerara K, Bertolino P, Ragon M, Tavera R, Lopez-Archilla AI, Lopez-Garcia P. 2016. Comparative metagenomics unveils functions and genome features of microbialite-associated communities along a depth gradient. Environ Microbiol 18:4990-5004.

53. Rasuk MC, Fernandez AB, Kurth D, Contreras M, Novoa F, Poire D, Farias ME. 2016. Bacterial Diversity in Microbial Mats and Sediments from the Atacama Desert. Microb Ecol 71:44-56.
54. Noda S, Hongoh Y, Sato T, Ohkuma M. 2009. Complex coevolutionary history of symbiotic Bacteroidales bacteria of various protists in the gut of termites. BMC Evol Biol 9:158.
55. Steichen SA, Gao S, Waller P, Brown JK. 2020. Association between algal productivity and phycosphere composition in an outdoor *Chlorella sorokiniana* reactor based on multiple longitudinal analyses. Microb Biotechnol 13:1546-1561.
56. Podosokorskaya OA, Kadnikov VV, Gavrilov SN, Mardanov AV, Merkel AY, Karnachuk OV, Ravin NV, Bonch-Osmolovskaya EA, Kublanov IV. 2013. Characterization of Melioribacter roseus gen. nov., sp. nov., a novel facultatively anaerobic thermophilic cellulolytic bacterium from the class Ignavibacteria, and a proposal of a novel bacterial phylum Ignavibacteriae. Environ Microbiol 15:1759-1771.
57. Thiel V, Garcia Costas AM, Fortney NW, Martinez JN, Tank M, Roden EE, Boyd ES, Ward DM, Hanada S, Bryant DA. 2019. “Candidatus Thermonerobacter thiotrophicus,” A Non-phototrophic Member of the Bacteroidetes/Chlorobi With Dissimilatory Sulfur Metabolism in Hot Spring Mat Communities. Front Microbiol 9.
58. Castelle CJ, Brown CT, Anantharaman K, Probst AJ, Huang RH, Banfield JF. 2018. Biosynthetic capacity, metabolic variety and unusual biology in the CPR and DPANN radiations. Nat Rev Microbiol 16:629-645.
59. Chaudhari NM, Overholt WA, Figueroa-Gonzalez PA, Taubert M, Bornemann TLV, Probst AJ, Hölzer M, Marz M, Küsel K. 2021. The economical lifestyle of CPR bacteria in groundwater allows little preference for environmental drivers. bioRxiv doi:10.1101/2021.07.28.454184:2021.07.28.454184.
60. Tian R, Ning D, He Z, Zhang P, Spencer SJ, Gao S, Shi W, Wu L, Zhang Y, Yang Y, Adams BG, Rocha AM, Detienne BL, Lowe KA, Joyner DC, Klingeman DM, Arkin AP, Fields MW, Hazen TC, Stahl DA, Alm EJ, Zhou J. 2020. Small and mighty: adaptation of superphylum Patescibacteria to groundwater environment drives their genome simplicity. Microbiome 8:51.
61. Moreira D, Zivanovic Y, López-Archilla AI, Iniesto M, López-García P. 2021. Reductive evolution and unique predatory mode in the CPR bacterium *Vampirococcus lugosii*. Nature Communications 12:2454.

62. Langwig MV, De Anda V, Dombrowski N, Seitz KW, Rambo IM, Greening C, Teske AP, Baker BJ. 2021. Large-scale protein level comparison of Deltaproteobacteria reveals cohesive metabolic groups. The ISME Journal doi:10.1038/s41396-021-01057-y.
63. Worm P, Koehorst JJ, Visser M, Sedano-Nunez VT, Schaap PJ, Plugge CM, Sousa DZ, Stams AJ. 2014. A genomic view on syntrophic versus non-syntrophic lifestyle in anaerobic fatty acid degrading communities. Biochim Biophys Acta 1837:2004-2016.
64. Pérez J, Moraleda-Muñoz A, Marcos-Torres FJ, Muñoz-Dorado J. 2016. Bacterial predation: 75 years and counting! Environ Microbiol 18:766-79.
65. Li L, Huang D, Hu Y, Rudling NM, Canniffe DP, Wang F, Wang Y. 2023. Globally distributed Myxococcota with photosynthesis gene clusters illuminate the origin and evolution of a potentially chimeric lifestyle. Nat Commun 14:6450.
66. Armbrecht L, Weber ME, Raymo ME, Peck VL, Williams T, Warnock J, Kato Y, Hernández-Almeida I, Hoem F, Reilly B, Hemming S, Bailey I, Martos YM, Gutjahr M, Percuoco V, Allen C, Brachfeld S, Cardillo FG, Du Z, Fauth G, Fogwill C, Garcia M, Glüder A, Guitard M, Hwang JH, Iizuka M, Kenlee B, O'Connell S, Pérez LF, Ronge TA, Seki O, Tauxe L, Tripathi S, Zheng X. 2022. Ancient marine sediment DNA reveals diatom transition in Antarctica. Nat Commun 13:5787.
67. Iniesto M, Moreira D, Benzerara K, Reboul G, Bertolino P, Tavera R, López-García P. 2022. Planktonic microbial communities from microbialite-bearing lakes sampled along a salinity-alkalinity gradient. Limnol Oceanogr 67:2718-2733.
68. Galindo LJ, López-García P, Torruella G, Karpov S, Moreira D. 2021. Phylogenomics of a new fungal phylum reveals multiple waves of reductive evolution across Holomycota. Nat Commun 12:4973.
69. Hess S, Suthaus A. 2022. The Vampyrellid Amoebae (Vampyrellida, Rhizaria). Protist 173:125854.
70. Bass D, Tikhonenkov DV, Foster R, Dyal P, Janouškovec J, Keeling PJ, Gardner M, Neuhauser S, Hartikainen H, Mylnikov AP, Berney C. 2018. Rhizarian 'Novel Clade 10' Revealed as Abundant and Diverse Planktonic and Terrestrial Flagellates, including Aquavolon n. gen. J Eukaryot Microbiol 65:828-842.
71. Hong J, Luesch H. 2012. Largazole: from discovery to broad-spectrum therapy. Nat Prod Rep 29:449-56.
72. Nemergut DR, Schmidt SK, Fukami T, O'Neill SP, Bilinski TM, Stanish LF, Knelman JE, Darcy JL, Lynch RC, Wickey P, Ferrenberg S. 2013. Patterns and processes of microbial community assembly. Microbiol Mol Biol Rev 77:342-56.

73. Foster RA, Zehr JP. 2019. Diversity, Genomics, and Distribution of Phytoplankton-Cyanobacterium Single-Cell Symbiotic Associations. Annu Rev Microbiol 73:435-456.
74. Schvarcz CR, Wilson ST, Caffin M, Stancheva R, Li Q, Turk-Kubo KA, White AE, Karl DM, Zehr JP, Steward GF. 2022. Overlooked and widespread pennate diatom-diazotroph symbioses in the sea. Nat Commun 13:799.
75. Chen MY, Teng WK, Zhao L, Han BP, Song LR, Shu WS. 2022. Phylogenomics Uncovers Evolutionary Trajectory of Nitrogen Fixation in Cyanobacteria. Mol Biol Evol 39.
76. Yancey CE, Mathiesen O, Dick GJ. 2023. Transcriptionally active nitrogen fixation and biosynthesis of diverse secondary metabolites by Dolichospermum and Aphanizomenon-like Cyanobacteria in western Lake Erie Microcystis blooms. Harmful Algae 124:102408.
77. Paerl HW, Pinckney JL. 1996. A Mini-review of Microbial Consortia: Their Roles in Aquatic Production and Biogeochemical Cycling. Microb Ecol 31:225-47.
78. Gogotov IN. 1978. Relationships in hydrogen metabolism between hydrogenase and nitrogenase in phototrophic bacteria. Biochimie 60:267-75.
79. Zeng Y, Nupur, Wu N, Madsen AM, Chen X, Gardiner AT, Koblížek M. 2020. Gemmatimonas groenlandica sp. nov. Is an Aerobic Anoxygenic Phototroph in the Phylum Gemmatimonadetes. Front Microbiol 11:606612.
80. Mujakić I, Andrei A-Ş, Shabarova T, Fecskeová Lívia K, Salcher Michaela M, Piwosz K, Ghai R, Koblížek M, Hallam Steven J. 2021. Common presence of phototrophic Gemmatimonadota in temperate freshwater lakes. mSystems 6:e01241-20.
81. Hess S. 2017. Description of *Hyalodiscus flabellus* sp. nov. (Vampyrellida, Rhizaria) and Identification of its Bacterial Endosymbiont, "*Candidatus* Megaira polyxenophila" (Rickettsiales, Alphaproteobacteria). Protist 168:109-133.
82. van Niel CB. 1949. The ‘Delft School’ and the rise of general microbiology. Bacteriol Rev 13:161–174.
83. de Wit R, Bouvier T. 2006. 'Everything is everywhere, but, the environment selects'; what did Baas Becking and Beijerinck really say? Environ Microbiol 8:755-758.
84. Uritskiy G, Munn A, Dailey M, Gelsinger DR, Getsin S, Davila A, McCullough PR, Taylor J, DiRuggiero J. 2020. Environmental Factors Driving Spatial Heterogeneity in Desert Halophile Microbial Communities. Front Microbiol 11:578669.

85. Belilla J, Moreira D, Jardillier L, Reboul G, Benzerara K, López-García JM, Bertolino P, López-Archilla AI, López-García P. 2019. Hyperdiverse archaea near life limits at the polyextreme geothermal Dallol area. Nature Ecol Evol 3:1552–1561.
86. Sauvadet AL, Gobet A, Guillou L. 2010. Comparative analysis between protist communities from the deep-sea pelagic ecosystem and specific deep hydrothermal habitats. Environ Microbiol 12:2946-2964.
87. Takai K, Nakamura K. 2011. Archaeal diversity and community development in deep-sea hydrothermal vents. Curr Opin Microbiol 14:282-291.
88. Zhou J, Ning D. 2017. Stochastic Community Assembly: Does It Matter in Microbial Ecology? Microbiol Mol Biol Rev 81.
89. Trivedi P, Leach JE, Tringe SG, Sa T, Singh BK. 2020. Plant–microbiome interactions: from community assembly to plant health. Nature Reviews Microbiology 18:607-621.
90. Estrela S, Vila JCC, Lu N, Bajić D, Rebolleda-Gómez M, Chang CY, Goldford JE, Sanchez-Gorostiaga A, Sánchez Á. 2022. Functional attractors in microbial community assembly. Cell Syst 13:29-42.e7.
91. Gralka M, Szabo R, Stocker R, Cordero OX. 2020. Trophic Interactions and the Drivers of Microbial Community Assembly. Curr Biol 30:R1176-r1188.
92. Cordero OX, Datta MS. 2016. Microbial interactions and community assembly at microscales. Curr Opin Microbiol 31:227-234.
93. Bonelli C, Dorador C. 2021. Endangered Salares: micro-disasters in Northern Chile. Tapuya: Latin American Science, Technology and Society doi:10.1080/25729861.2021.1968634:1968634.

FIGURE LEGENDS

Figure 1. Map of the study area indicating the sampling zones. Pictures of the sampling zones H0 to H4 are shown.

Figure 2. Barplots showing the microbial community composition based of 16S/18S rRNA gene amplicon sequencing in samples from the Salar de Huasco. A, prokaryotic communities. B, eukaryotic communities. Samples labeled W, BF, M and S correspond, respectively, to plankton, biofilm, microbial mat and underlying sediment (Table 2).

Figure 3. Nonmetric Multidimensional Scaling analysis of microbial communities studied in the Salar de Huasco. A, prokaryotic communities. B, eukaryotic communities. Vectors of major measured environmental parameters (Table S1) are included; significant parameters are shown with red arrows. TDS, total dissolved solids.

Figure 4. Results of Mantel tests showing correlations of microbial communities with abiotic and biotic parameters. A-B, correlations between prokaryotic (A) and eukaryotic (B) community structure (Bray-Curtis dissimilarities) as a function of cumulative abiotic environmental parameters. C-D, correlations between the photosynthetic (C) and non-photosynthetic (D) component of eukaryotic communities as a function of cumulative abiotic environmental parameters. E-F, correlation between prokaryotic community structure and photosynthetic (E) and non-photosynthetic (F) fractions of eukaryotic microbial communities.

Figure 5. Co-occurrence networks of prokaryotic and eukaryotic members of mat and sediment samples from Salar de Huasco. Only the top 30% of positive correlations between prokaryotic and eukaryotic ASVs are displayed.

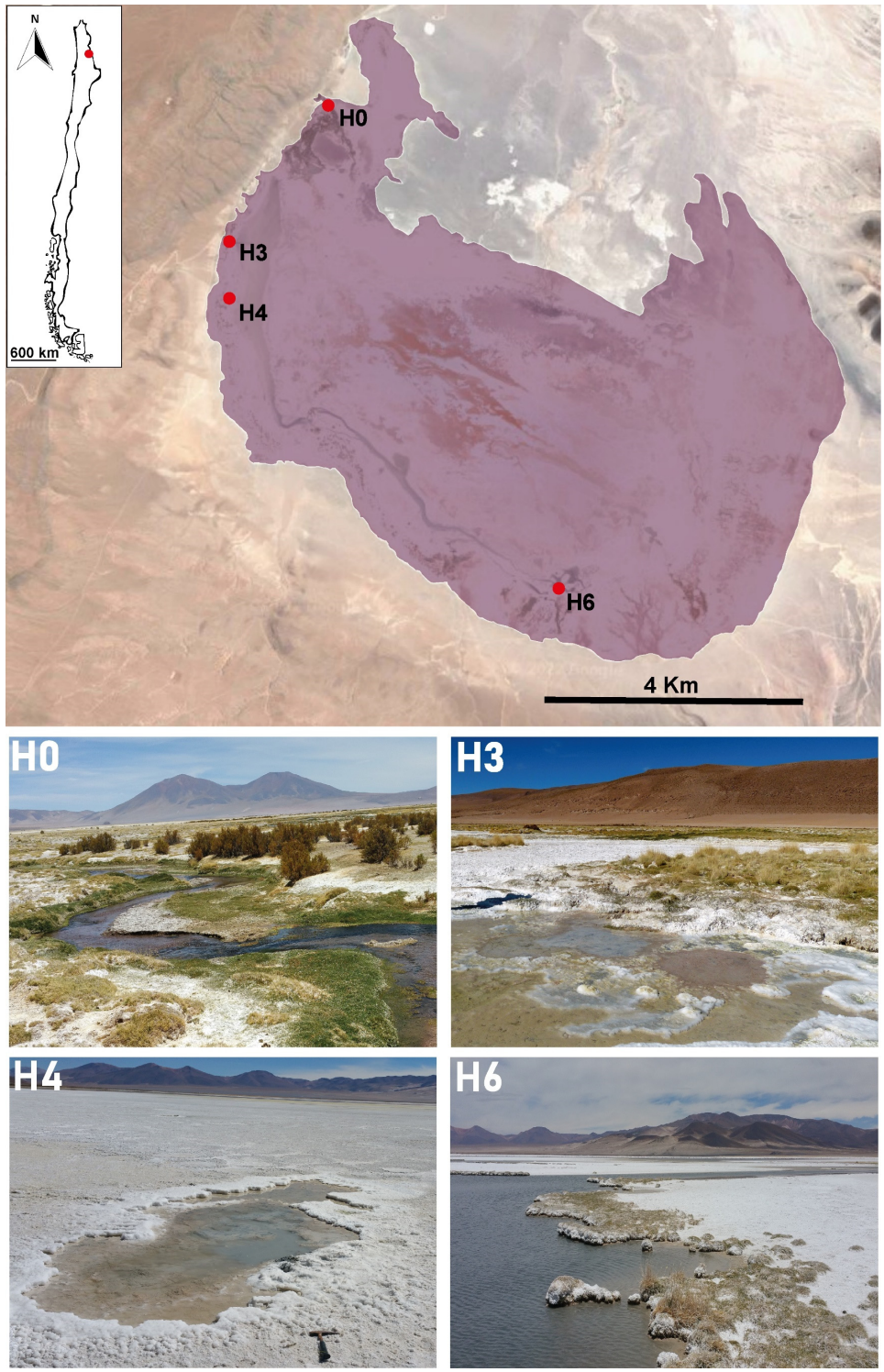

Figure 1. Cubillos et al.

Figure 2. Cubillos et al.

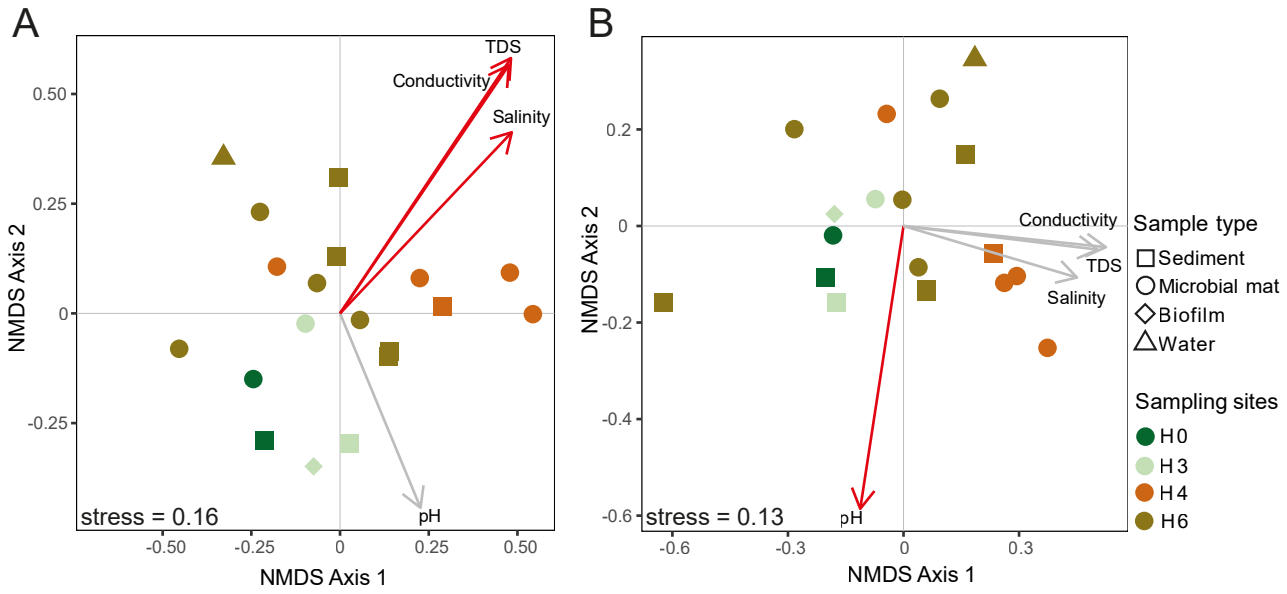

Figure 3. Cubillos et al.

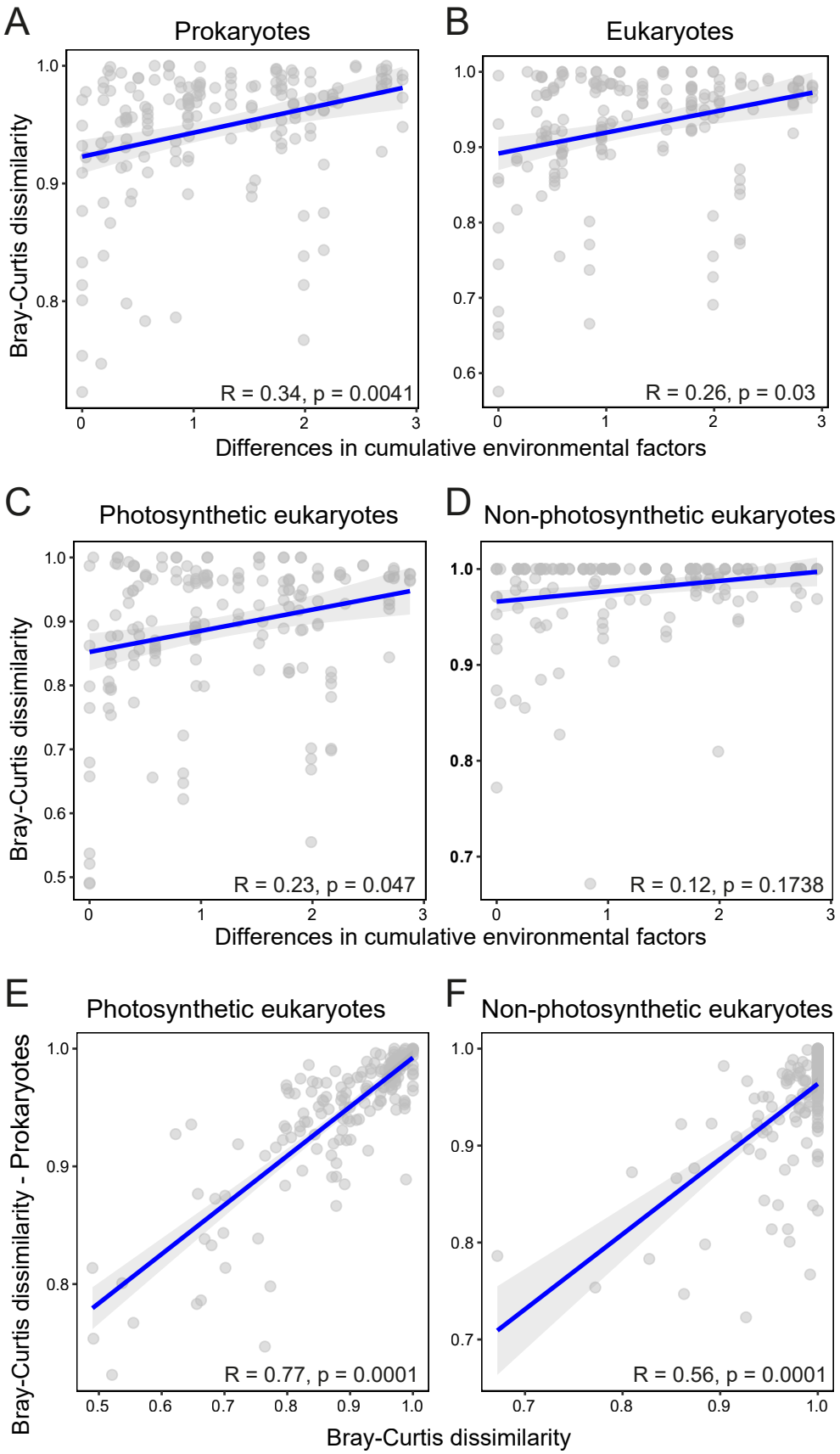

Figure 4. Cubillos et al.

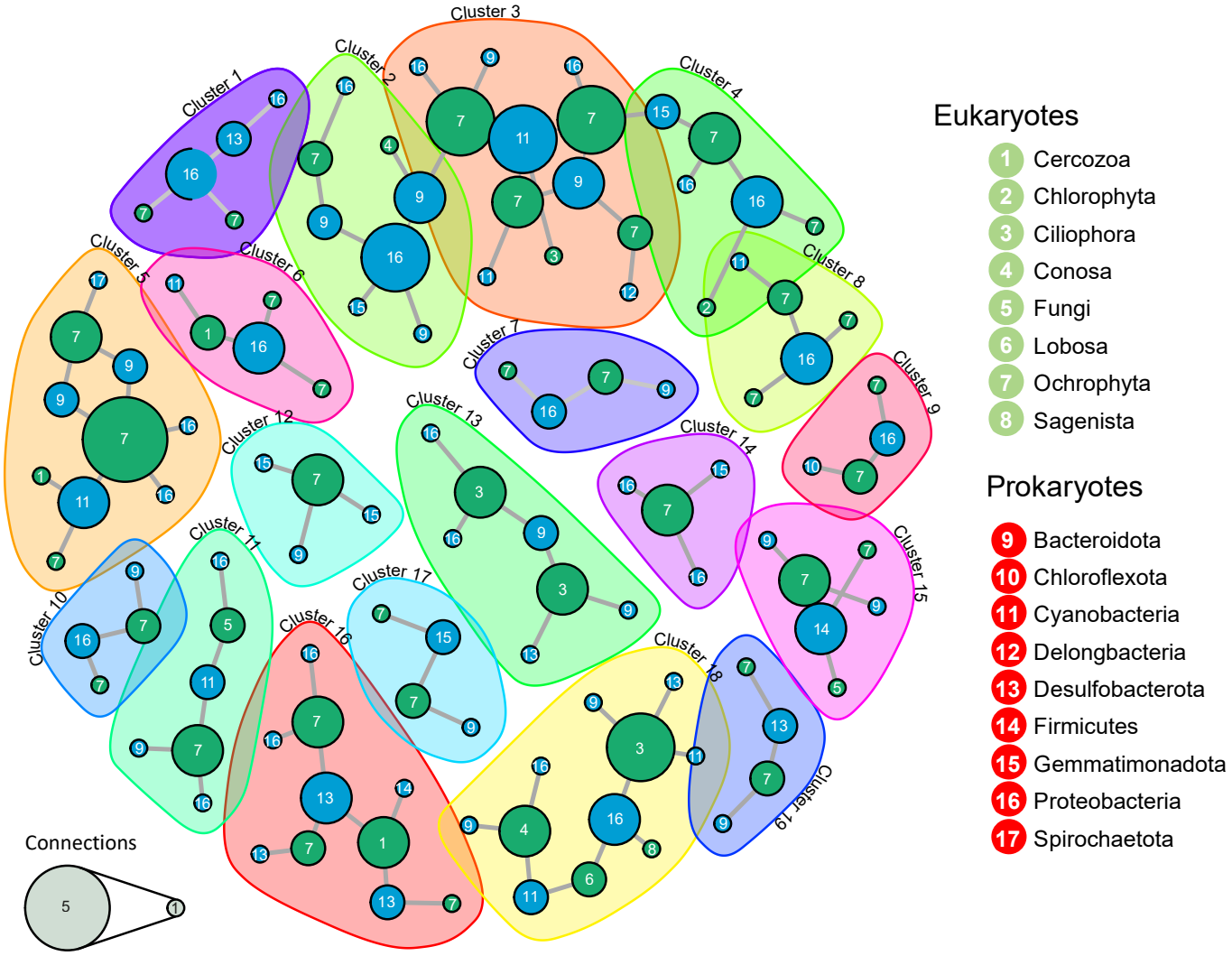

Figure 5. Cubillos et al.